

Lattice Ginzburg-Landau model of a ferromagnetic p -wave pairing phase in superconducting materials and an inhomogeneous coexisting state

Akihiro Shimizu, Hidetoshi Ozawa, and Ikuo Ichinose

Department of Applied Physics, Nagoya Institute of Technology Nagoya 466-8555, Japan

Tetsuo Matsui

Department of Physics, Kinki University, Higashi-Osaka 577-8502, Japan

(Received 19 May 2011; revised manuscript received 15 March 2012; published 27 April 2012)

We study the interplay of the ferromagnetic (FM) state and the p -wave superconducting (SC) state observed in several materials such as UCoGe and URhGe in a totally nonperturbative manner. To this end, we introduce a lattice Ginzburg-Landau model that is a genuine generalization of the phenomenological Ginzburg-Landau theory proposed previously in the continuum and also a counterpart of the lattice gauge Higgs model for the s -wave SC transition, and study it numerically by Monte Carlo simulations. The obtained phase diagram has qualitatively the same structure as that of UCoGe in the region where the two transition temperatures satisfy $T_{\text{FM}} > T_{\text{SC}}$. For $T_{\text{FM}}/T_{\text{SC}} < 0.7$, we find that the coexisting region of FM and SC orders appears only near the surface of the lattice, which describes an inhomogeneous FMSC coexisting state.

DOI: [10.1103/PhysRevB.85.144524](https://doi.org/10.1103/PhysRevB.85.144524)

PACS number(s): 74.20.-z, 74.25.Dw, 74.25.Ha

I. INTRODUCTION

In the last decade, superconducting (SC) materials coexisting with ferromagnetic (FM) long-range orders have been found and are of intensive interest. In UGe₂ (Ref. 1) and URhGe (Ref. 2), a SC state appears only within the FM state in the pressure-temperature (P - T) phase diagram, whereas in UCoGe,³ the SC state exists both in the FM and paramagnetic states.⁴ Phenomenological models of FMSC materials were proposed^{5,6} soon after their discovery. The most important observation in those studies is that the FMSC state is a spin-triplet p -wave state of electron pairs.⁷

In this paper, we propose a lattice model for describing FMSC materials and investigate it by numerical methods.⁸ The model contains a vector potential (i.e., gauge field) to describe a FM order parameter (magnetization) and also a SC order parameter, i.e., Cooper-pair field for the p -wave SC state. These two physical variables couple with each other as the Cooper pair bears the electric charge $2e$. Finite magnetization inside the material tends to induce vortices of the Cooper-pair field and destabilize the SC state. In this sense, the FMSC state is a result of frustration.

Introduction of the spatial lattice in the present model has several advantages over the Ginzburg-Landau (GL) theory in the continuum space:^{5,6,9} (i) it reflects the lattice structure of the real materials, (ii) it works as a regularization of vortex configurations because the energy of these topological excitations becomes finite, and (iii) it allows us to make a nonperturbative study by means of Monte Carlo simulations in which contributions from all the field configurations including topologically nontrivial excitations are taken into account, and so the obtained results are quite reliable. In this sense, this study is complementary to the previous analytical studies employing perturbative and mean-field-like approximations.^{5,6,9}

This paper is organized as follows. In Sec. II, we introduce the lattice GL model, which is derived from the previously proposed GL theory in the continuum. Detailed discussion on the physical properties of the model is also given there.

In Sec. II A, we present a brief review on the lattice gauge model for the SC state. This review may be useful to make this paper readable for condensed matter physicists who are not familiar with the models of the SC state on the lattice. In Sec. III, we present results of the numerical study. The phase structure of the model is clarified by calculating specific heat, FM correlation function, shielding mass of magnetic field, etc. We also study behavior of vortices in a constant magnetic field in the present model in order to obtain an intuitive picture of the Meissner state. Section IV is devoted for conclusion.

II. LATTICE MODEL FOR FMSC STATE

A. Lattice gauge Higgs model for SC transition

In this section, we review a typical lattice model to describe the conventional SC transition, which is called the U(1) gauge Higgs model (or the Abelian Higgs model). The reader who is familiar with this subject can skip this section and go to Sec. II B.

Let us start with the GL theory of s -wave SC state in the three-dimensional (3D) continuum space. Its free-energy density is given by

$$f_{s\text{GL}} = |D_\mu \psi|^2 + \alpha(T - T_c^0)|\psi|^2 + \lambda|\psi|^4 + \frac{1}{8e^2}(\text{rot}\vec{A}^{\text{em}})^2, \quad (2.1)$$

$$D_\mu = \partial_\mu - iA_\mu^{\text{em}},$$

where ψ is the complex scalar field for s -wave Cooper pairs, \vec{A}^{em} is the vector potential ($\times 2e$) for fluctuating electromagnetic field, D_μ is the covariant derivative in the μ th direction ($\mu = 1, 2, 3$), T_c^0 is the bare critical temperature (T) of SC transition, e is the elementary charge, and α and λ are positive T -independent parameters.

The lattice-field model corresponding to the GL theory (2.1) is defined by giving its free energy (or the action including the

inverse temperature) F as follows:

$$F = -\frac{K}{2} \sum_{x,\mu} (\psi_{x+\mu}^* U_{x\mu} \psi_x + \text{c.c.}) + F_\psi + F_A, \quad (2.2)$$

$$F_\psi = \sum_x (\sigma |\psi_x|^2 + \lambda |\psi_x|^4), \quad U_{x\mu} = \exp(i A_{x\mu}^{\text{em}}), \quad (2.3)$$

where x is the site of the 3D lattice, ψ_x is a complex SC order-parameter field defined on the site x , and we use μ also as the unit vector in the μ th direction. ψ_x is sometimes called Higgs field because it is a complex scalar field. $A_{x\mu}^{\text{em}}$ is a real electromagnetic field ($\times -2e$) put on the link $(x, x+\mu)$. F_A is the free energy of the electromagnetic field and has the following two versions. One is the compact version

$$F_A = -\frac{1}{8e^2} \sum_{x,\mu < \nu} (U_{x\nu}^* U_{x+\nu,\mu}^* U_{x+\mu,\nu} U_{x\mu} + \text{c.c.}),$$

$$A_{x\mu}^{\text{em}} \in (-\pi, \pi), \quad (2.4)$$

and the other is the noncompact version

$$F_A = \frac{1}{8e^2} \sum_{x,\mu < \nu} (\nabla_\mu A_{x\nu}^{\text{em}} - \nabla_\nu A_{x\mu}^{\text{em}})^2,$$

$$A_{x\mu}^{\text{em}} \in (-\infty, \infty), \quad (2.5)$$

where ∇_μ is the lattice difference operator such that

$$\nabla_\mu f_x \equiv f_{x+\mu} - f_x. \quad (2.6)$$

These two F_A are distinguished by having the periodicity under $A_{x\mu}^{\text{em}} \rightarrow A_{x\mu}^{\text{em}} + 2\pi$ or not. We note that F of Eq. (2.2) is invariant under the local U(1) gauge transformation

$$\psi_x \rightarrow \psi'_x = \exp(i\lambda_x) \psi_x,$$

$$A_{x\mu}^{\text{em}} \rightarrow A'_{x\mu} = A_{x\mu}^{\text{em}} + \lambda_{x+\mu} - \lambda_x, \quad (2.7)$$

$$U_{x\mu} \rightarrow U'_{x\mu} = \exp(i\lambda_{x+\mu}) U_{x\mu} \exp(-i\lambda_x),$$

where λ_x is a site-dependent real variable.

Let us first consider the pure gauge system described by the energy F_A alone. In the case in which fluctuations of the vector potential $A_{x\mu}^{\text{em}}$ are small, the above two versions belong to the same universality class, i.e., the system is in the Coulomb phase. This is because F_A of Eq. (2.4) approaches to (2.5) due to the relation

$$U_{x\nu}^* U_{x+\nu,\mu}^* U_{x+\mu,\nu} U_{x\mu} + \text{c.c.} = 2 \cos \theta_{x\mu\nu},$$

$$\theta_{x\mu\nu} \equiv \nabla_\mu A_{x\nu}^{\text{em}} - \nabla_\nu A_{x\mu}^{\text{em}}, \quad (2.8)$$

$$\cos \theta_{x\mu\nu} \simeq 1 - \frac{1}{2} \theta_{x\mu\nu}^2 \quad \text{for small } \theta_{x\mu\nu}.$$

For large fluctuations of vector potentials, the compact version generally allows topologically nontrivial excitations such as magnetic monopoles and may exhibit another phase called the confinement phase, which is not allowed in the noncompact version.

Next, we consider the case in which the magnetic field is switched off by setting $A_{x\mu}^{\text{em}} = 0$. Then, the system (2.2) is reduced to the $|\phi|^4$ theory. In the 3D $|\phi|^4$ theory, there exists a second-order phase transition accompanying the spontaneous symmetry breaking of the global U(1) symmetry under the phase rotation $\psi_x \rightarrow \exp(i\theta) \psi_x$. This broken phase is called the Higgs phase and corresponds to the SC phase. In the limit of $\lambda \rightarrow \infty$ with the ratio σ/λ kept fixed to a finite negative value,

the system reduces to the so-called XY model defined with $|\psi_x| = \sqrt{-\sigma/2\lambda}$, which is well known to exhibit a second-order transition as K is varied. This limit corresponds to the London limit of superconductivity (or superfluidity), and the phase transition in the $|\phi|^4$ theory for large λ and that of the XY model belong to the same universality class. Even in this simplified model, the detailed critical behavior at the phase transition is *different from* that described by the mean-field theory (MFT).

Finally, let us turn on the vector potential $A_{x\mu}^{\text{em}}$. In the continuum, it is shown¹⁰ that the second-order transition for $\vec{A}^{\text{em}} = 0$ is changed to a first-order one as the GL parameter $\kappa \propto \lambda/e^2$ is decreased. On the lattice, the compact version of the system is studied in Ref. 11 and it is verified that the phase transition takes place as one varies K with fixed κ . More precisely, the phase transition is of first order for small κ and becomes second order for large κ as in the model defined in the continuum.¹⁰ Here, we should note that the study in Ref. 12 shows that the critical behavior of the second-order transition near the London limit is *not* in the same universality class as the 3D XY model due to the gauge-field fluctuations.

The noncompact lattice version is also studied in the London limit in Ref. 13. The corresponding energy is obtained from Eq. (2.2) by making the replacement

$$\frac{K}{2} \sum_{x,\mu} (\psi_{x+\mu}^* U_{x\mu} \psi_x + \text{c.c.}) \rightarrow \frac{\tilde{K}}{2} \sum_{x,\mu} (e^{-i\varphi_{x+\mu}} U_{x\mu} e^{i\varphi_x} + \text{c.c.}), \quad (2.9)$$

where φ_x is the *phase* of the Cooper-pair (Higgs) field ψ_x , and neglecting F_ψ in Eq. (2.3) because it becomes a constant. In Ref. 13, this U(1) gauge Higgs model on the four-dimensional lattice is studied for large $1/e^2$, which exhibits a second-order transition as \tilde{K} is varied. This is consistent with the fact that, in the limit of $1/e^2 \rightarrow \infty$, the system reduces to the four-dimensional (4D) XY model. This phase transition is induced by the condensation of vortex excitations in φ_x . In the terminology of XY spin model, the XY spin $\vec{S}_x \equiv (\cos \varphi_x, \sin \varphi_x)^t$ has a long-range order $\langle \vec{S}_x \rangle \neq 0$ in the Higgs phase, whereas $\langle \vec{S}_x \rangle = 0$ in the disordered phase due to the strong fluctuations of its angle φ_x .

Then, it is useful to rewrite the system in terms of topological excitations such as vortices and monopoles. In the London limit of Eq. (2.2), the duality transformation can be performed,^{13,14} and the free energy is expressed by the integer-valued vortex line-element variables $J_{\vec{x}\mu}$ and the integer-valued monopole-density variables $Q_{\vec{x}} \equiv \nabla_\mu J_{\vec{x}\mu}$ sitting on the dual lattice (\vec{x} denotes its site) as

$$F_v = 4\pi^2 \tilde{K} \sum_{\vec{x}, \vec{y}} \left(\sum_\mu J_{\vec{x}\mu} J_{\vec{y}\mu} + \frac{1}{m_0^2} Q_{\vec{x}} Q_{\vec{y}} \right) D_{\vec{x}, \vec{y}}, \quad (2.10)$$

$$D_{\vec{x}, \vec{y}} \simeq \frac{\exp(-m_0 r)}{m_0 r}, \quad r = |\vec{x} - \vec{y}|, \quad m_0^2 = 8\tilde{K} e^2,$$

where $D_{\vec{x}, \vec{y}}$ is the 3D lattice Green's function with mass m . As explained in the Introduction, there appear no singularities in F_v of Eq. (2.10).

For the noncompact version of the gauge system, it is shown in Ref. 13 that no monopoles exist $Q_{\vec{x}} = 0$ and only the

closed vortex loops that satisfy $\sum_{\mu} \nabla_{\mu} J_{\bar{x}\mu} = 0$ are allowed as expected. In the Coulomb phase with lower \tilde{K} , these vortex loops condense, while in the Higgs phase with higher \tilde{K} vortex loops are suppressed.

On the other hand, for the compact version,¹⁴ open vortex strings may appear and a monopole should locate at every end of an open string such that $\sum_{\mu} \nabla_{\mu} J_{\bar{x}\mu} = Q_{\bar{x}} \neq 0$. Condensation of these monopoles may imply sufficiently large fluctuations of \vec{A}^{em} and drive the system into the confinement phase.¹⁵ In fact, in the 3D compact case, the system is known to stay always in the confinement phase for any \tilde{K} .^{15,16} In the 4D compact case, there is a gauge transition from the confinement phase to the Coulomb phase as $1/e^2$ increases and a Higgs transition from the Coulomb phase to the Higgs phase as \tilde{K} increases.¹⁷ Here, let us comment on the 3D multicomponent Higgs model in the compact version with N Higgs fields in the London limit.¹⁸ In contrast to the above 3D model with $N = 1$, the model with $N \geq 2$ supports the Higgs phase due to the extra phase degrees of freedom that are free from coupling to the gauge field.

The above discussion clearly shows that the SC phase transitions do take place even in the London limit for the gauge Higgs model both for the noncompact gauge version with $N = 1$ and for the compact version with $N \geq 2$, and topological excitations of SC order parameters, vortices, play an important role for that.

Usually, the genuine transition temperature T_c of the system (2.1) is lower than the bare critical temperature T_c^0 due to fluctuation effect. The radial degrees of freedom of ψ_x may certainly contribute such renormalization of T_c , but should not change the universality class of the continuous phase transition that we are to study because their fluctuations are massive.

In the rest of this paper, we shall study the FMSC state by starting with a lattice model corresponding to Eq. (2.2) in the London limit, in which vortices are expected to be generated spontaneously, and therefore nonperturbative study is indispensable for the investigation.

B. GL theory in the continuum

In the proposed GL theory^{5,6} for the FMSC materials in the 3D continuum space at finite T , the free-energy density f_{GL} for the SC state measured from the normal state is given as

$$\begin{aligned} f_{\text{GL}} = & K \sum_{\mu} (D_{\mu} \vec{\psi})^* \cdot (D_{\mu} \vec{\psi}) + \alpha (T - T_{\text{SC}}^0) \vec{\psi}^* \cdot \vec{\psi} \\ & + \lambda (\vec{\psi}^* \cdot \vec{\psi})^2 + K' \sum_{\mu} (\partial_{\mu} \vec{m})^2 + (T - T_{\text{FM}}^0) \vec{m}^2 \\ & + \alpha_f (\vec{m}^2)^2 + f_Z, \end{aligned} \quad (2.11)$$

$$\begin{aligned} D_{\mu} = & \partial_{\mu} - 2ieA_{\mu}, \quad f_Z = -J\vec{m} \cdot \vec{S}, \\ \vec{m} = & \vec{\nabla} \times \vec{A}, \quad \vec{S} = i\vec{\psi}^* \times \vec{\psi}, \end{aligned}$$

with the spatial direction index $\mu = 1, 2, 3$. The three-component complex field $\vec{\psi} = (\psi_1, \psi_2, \psi_3)^t$ is the spin-triplet SC order parameter, i.e., the Cooper-pair field [we omit the spatial coordinate x in the field $\vec{\psi}(x)$, etc.]. $\vec{\psi}$ is proportional to the \vec{d} vector in the spin space $\vec{\psi} \propto \vec{d}$ and also the wave function of the p -wave SC state in the real space as a result of the spin-orbit coupling. In terms of $\vec{\psi}$, the magnetization (spin

and angular momentum) \vec{S} of Cooper pairs is expressed as in Eq. (2.11).⁵ The FM order is described by the magnetization field \vec{m} of electrons that *do not* participate in the SC state. T_{SC}^0 and T_{FM}^0 are the *bare* critical temperatures of SC and FM transitions, respectively. Because \vec{m} satisfies $\vec{\nabla} \cdot \vec{m} = 0$, it can be expressed in terms of the vector potential \vec{A} as $\vec{m} = \text{rot} \vec{A}$. Because the Cooper-pair field bears the electric charge $-2e$, it couples with \vec{A} minimally via the covariant derivative D_{μ} reflecting the electromagnetic gauge invariance. We note that this vector potential \vec{A} is *not* the one for the external electromagnetic field $A_{x\mu}^{\text{em}}$ in Eq. (2.2). f_Z is the Zeeman coupling term between \vec{S} and \vec{m} . It may induce the FMSC state⁵ in which $\langle \vec{m} \rangle \neq 0, \langle \vec{S} \rangle \neq 0$.

The GL theory (2.11) and the related ones have been studied so far by means of MFT-type methods.⁹ However, the gauge coupling between \vec{A} and $\vec{\psi}$ makes a simple MF approximation assuming, e.g., a constant SC order parameter and ignoring topologically nontrivial fluctuations unreliable for the description of the FMSC state. This is also indicated as we explained for the model of s -wave SC state Eqs. (2.1) and (2.2). Therefore, f_{GL} in Eq. (2.11) is a kind of *frustrated system of the AF and SC*. We dare to use the word ‘‘frustrated’’ here. This is because the case with a finite magnetization $\vec{m} \neq 0$ corresponds to the case with a nonvanishing external magnetic field: a well-known case of frustration. In fact, the phase of matter field there should acquire a finite additional phase when it is rotated along a closed loop and so the phase is not determined uniquely except for an integer magnetic flux inside the loop. In other words, vortices are to be generated because of the presence of the nonvanishing magnetization.

It is of course important to study the set of GL equations derived from f_{GL} in Eq. (2.11). The GL equations should be solved self-consistently to obtain $\vec{\psi}(x)$ and $A_{\mu}(x)$. In the FM phase, $\vec{\psi}(x)$ describes multivortex states and the vector potential $A_{\mu}(x)$ is determined by the locations of vortices in addition to the other terms in f_{GL} , including the magnetization $\vec{m}(x)$.

In this paper, we shall introduce a GL theory defined on a cubic lattice, which is a discretized version of Eq. (2.11), and study its phase structure, etc., by means of the Monte Carlo simulations. In this approach, all relevant fluctuations of $\vec{\psi}$ and A_{μ} are taken into account. Some related lattice model describing a two-component SC was studied and interesting results were obtained.¹⁹ The above two approaches, MFT of the GL solutions and the numerical study of the GL theory, are complementary and not exclusive of each other.

C. Derivation of the lattice model

As announced in Sec. I, we introduce an effective lattice gauge model based on the GL theory in the continuum (2.11) by making a couple of simplifications. We stress that topological defects such as vortices are allowed on the lattice without introducing an additional short-distance cutoff for vortex cores. This point is quite important because it is expected that such nontrivial excitations are generated in the FMSC phase.

As the first step of simplification, we consider the ‘‘London limit’’ of $\vec{\psi}$ such that $\vec{\psi}^* \cdot \vec{\psi} = \text{const.}$ determined by minimizing f_{GL} of Eq. (2.11), neglecting its radial fluctuations.

As discussed in Sec. II A for the s -wave SC model, this is legitimate because the phase degrees of freedom of $\vec{\psi}$ play an essential role for (in)stability of the SC state.

Second, the FMSC materials have a FM easy axis, which we choose as the z direction ($\mu = 3$).²⁰ Then, the Zeeman coupling f_Z prefers such that $\psi_{\uparrow\uparrow} \propto \psi_1 + i\psi_2$ or $\psi_{\downarrow\downarrow} \propto \psi_1 - i\psi_2$ takes large amplitude. In fact, as the Fermi surfaces of up- and down-spin electrons have different energies due to f_Z , the Cooper-pair amplitude of mixed spins $\psi_3 = \psi_{\uparrow\downarrow}$ is small.

Therefore, in the effective model, we ignore ψ_3 as in the previous studies^{5,7,20} and consider only the two-component complex field $(\psi_1, \psi_2)^t$ in the London limit

$$\begin{aligned} (\psi_1, \psi_2, \psi_3) &\rightarrow (\psi_1, \psi_2, 0) \quad \text{with} \\ |\psi_1|^2 + |\psi_2|^2 &= \frac{\alpha}{2\lambda}(T_{\text{SC}}^0 - T). \end{aligned} \quad (2.12)$$

Here, we introduce a two-component complex field z that is the normalized Cooper-pair field: $z = (z_1, z_2)^t$ satisfying

$$|z_1|^2 + |z_2|^2 = 1, \quad (2.13)$$

and from Eq. (2.12)

$$(\psi_1, \psi_2)^t = \sqrt{\frac{\alpha}{2\lambda}(T_{\text{SC}}^0 - T)} (z_1, z_2)^t. \quad (2.14)$$

We note that two-component complex variables satisfying Eq. (2.13) such as $z(x)$ is called a CP^1 (complex projective) field. In terms of $z(x)$, the first term of f_{GL} in Eq. (2.11) is given as

$$\frac{K\alpha}{2\lambda}(T_{\text{SC}}^0 - T) \sum_{\mu} (D_{\mu}z)^*(D_{\mu}z). \quad (2.15)$$

Now, let us consider the effective lattice model on the 3D cubic lattice. Its GL free-energy density f_x at the site x is given up to an irrelevant constant by

$$\begin{aligned} f_x &= -\frac{c_1}{2} \sum_{\mu=1}^3 \sum_{a=1}^2 (\bar{z}_{x+\mu,a} U_{x\mu} z_{xa} + \text{c.c.}) - c_2 \vec{m}_x^2 \\ &\quad - c_3 \vec{m}_x \cdot \vec{S}_x + c_4 (\vec{m}_x^2)^2 - c_5 \sum_{\mu} \vec{m}_x \cdot \vec{m}_{x+\mu}, \end{aligned} \quad (2.16)$$

$$U_{x\mu} \equiv \exp(iA_{x\mu}).$$

The five coefficients c_i ($i = 1 \sim 5$) in Eq. (2.16) are real non-negative parameters that are expected to distinguish various materials in various environments. $z_x = (z_{x1}, z_{x2})^t$ ($\sum_{a=1}^2 |z_{xa}|^2 = 1$) is the CP^1 variable at the site x and plays the role of SC order-parameter field. $U_{x\mu}$ is the exponentiated vector potential²¹ put on the link $(x, x + \mu)$. $\vec{m}_x = (m_{x1}, m_{x2}, m_{x3})^t$ is the magnetic field made out of $A_{x\mu}$ as

$$m_{x\mu} \equiv \sum_{\nu,\lambda=1}^3 \epsilon_{\mu\nu\lambda} \nabla_{\nu} A_{x\lambda}, \quad \nabla_{\nu} A_{x\lambda} \equiv A_{x+\nu,\lambda} - A_{x\lambda}. \quad (2.17)$$

\vec{m}_x serves as the FM order-parameter field. $\vec{S}_x = (0, 0, S_{x3})^t$ is an Ising-type spin vector of Cooper pairs made out of z_{xa} as

$$S_{x3} \equiv i(z_{x1}^* z_{x2} - z_{x2}^* z_{x1}) \propto |\psi_{\uparrow\uparrow}|^2 - |\psi_{\downarrow\downarrow}|^2. \quad (2.18)$$

As for the case of Eq. (2.7), f_x is invariant under a $U(1)$ gauge transformation

$$\begin{aligned} z_{xa} &\rightarrow z'_{xa} = \exp(i\lambda_x) z_{xa}, \\ U_{x\mu} &\rightarrow U'_{x\mu} = \exp(i\lambda_{x+\mu}) U_{x\mu} \exp(-i\lambda_x). \end{aligned} \quad (2.19)$$

We note that both \vec{m}_x and \vec{S}_x are gauge invariant.

The meaning of each term in f_x is as follows. The c_1 term describes a hopping of Cooper pairs. From Eq. (2.15), it is obvious that

$$c_1 \sim K\alpha\lambda^{-1}(T_{\text{SC}}^0 - T)a, \quad (2.20)$$

where a is the lattice spacing. At sufficiently large c_1 , the c_1 term may stabilize the phase of z_{xa} up to a gauge transformation, and then a *coherent condensation of the phase degrees of freedom of z_x induces the superconductivity*. The c_2 and c_4 terms are the quartic GL potential of \vec{m}_x and favor a finite amount of *local* magnetization $\langle \vec{m}_x \rangle \neq 0$ (note that we take $c_2 > 0$). Again, we note that these terms control intrinsic magnetization in contrast with F_A of Eq. (2.2) for the fluctuating but external magnetic field. The c_5 term enhances uniform configurations of \vec{m}_x , i.e., a FM long-range order signaled by a finite magnetization $\lim_{|x-x'|\rightarrow\infty} \langle \vec{m}_x \cdot \vec{m}_{x'} \rangle \neq 0$. The c_3 term is the Zeeman coupling, which favors collinear configurations of \vec{m}_x and \vec{S}_x , namely, the coexistence of ferromagnetism and superconductivity.

The partition function Z at T is given by the integral over a set of two fundamental fields z_{xa} and $A_{x\mu}$ as

$$\begin{aligned} Z &= \int [dz][dA] \exp(-\beta F), \quad \beta = T^{-1}, \quad F = \sum_x f_x, \\ [dz] &= \prod_x d^2 z_{x1} d^2 z_{x2} \delta(|z_{x1}|^2 + |z_{x2}|^2 - 1), \\ [dA] &= \prod_{x,\mu} dA_{x\mu}, \quad A_{x\mu} \in (-\infty, \infty). \end{aligned} \quad (2.21)$$

The coefficients c_i in f_x may have nontrivial T dependence as Eqs. (2.11) and (2.20) suggest. However, in this study we consider the response of the system by varying the “temperature” $T \equiv 1/\beta$ defined by β , an overall prefactor in Eq. (2.21), while keeping c_i fixed. This method corresponds to well-known studies such as the FM transition by means of the $O(3)$ nonlinear- σ model²² and the lattice gauge Higgs models discussed in Sec. II A, and sufficient to determine the critical temperatures. See later discussion leading to Eq. (3.6).

III. NUMERICAL STUDIES

A. FM and SC phase transitions and Meissner effect

For explicit procedures of our Monte Carlo simulations, we first prepare a 3D lattice of the size of $(2 + L + 2)^2 \times L$, namely, the lattice coordinates running as $x_1, x_2 = 0, \dots, L + 3$, $x_3 = 0, \dots, L - 1$. The extra width $2 + 2$ in the $\mu = 1, 2$ directions is introduced as a buffer zone in which the supercurrent is damped. The calculations of physical quantities are done in the central region R of the size L^3 to suppress the effects of the boundary. For the boundary condition, we choose the periodic boundary condition in the $\mu = 3$ direction. For the $\mu = 1, 2$ directions, we first note that the supercurrent density

$j_{x\mu}^{\text{SC}}$ on the lattice is expressed as

$$j_{x\mu}^{\text{SC}} \propto \text{Im} (\bar{z}_{x+\mu} U_{x\mu} z_x). \quad (3.1)$$

Then, we impose

$$\begin{aligned} z_{x+\mu} - U_{x\mu} z_x = 0 \quad \text{for} \quad & x = (0, x_2, x_3), \quad \mu = 1, \\ & x = (L + 2, x_2, x_3), \quad \mu = 1, \\ & x = (x_1, 0, x_3), \quad \mu = 2, \\ & x = (x_1, L + 2, x_3), \quad \mu = 2, \end{aligned} \quad (3.2)$$

whereas we impose the free boundary condition on $A_{x\mu}$ ($\mu = 1, 2$).

The above condition (3.2) is gauge invariant and assures us that $j_{x\mu}^{\text{SC}} = 0$ ($\mu = 1, 2$) on the boundary surfaces in the $\mu - 3$ plane; the supercurrent does not leak out of the SC material put in the region R . We note that this boundary condition for $A_{x\mu}$ enhances the third component of the FM order so that $\langle \vec{m}_x \rangle = (0, 0, m_3)^t$. This fact is traced back to our choice $\psi_3 = 0$ in Eq. (2.12) and reflects the experimental fact that the real FMSC materials exhibit the Ising-type anisotropy of the FM magnetization. Note also that the conventional periodic boundary condition for $A_{x\mu}$ in all the three directions implies $\sum_x \vec{m}_x = 0$ and the FM order can not exist.

We use standard Metropolis algorithm for the lattice size up to $L = 20$. The typical sweeps for measurement are $(30\,000 \sim 50\,000) \times 10$ and the acceptance ratio is 40% \sim 50%.

Explicitly, we calculate the internal energy U , the specific heat C of the central region R , the FM magnetization m_μ ,

$$\begin{aligned} U &= \frac{1}{L^3} \langle F' \rangle, \quad C = \frac{1}{L^3} \langle (F' - \langle F' \rangle)^2 \rangle, \quad F' = \sum_{x \in R} f_x, \\ m_\mu &\equiv \frac{1}{L^3} \left\langle \left\langle \sum_{x \in R} m_{x\mu} \right\rangle \right\rangle, \end{aligned} \quad (3.3)$$

and the normalized correlation functions

$$\begin{aligned} G_m(x - x_0) &= \langle \vec{m}_x \cdot \vec{m}_{x_0} \rangle / \langle \vec{m}_{x_0} \cdot \vec{m}_{x_0} \rangle, \\ G_S(x - x_0) &= \langle S_{x,3} S_{x_0,3} \rangle / \langle S_{x_0,3} S_{x_0,3} \rangle, \end{aligned} \quad (3.4)$$

where x_0 is chosen on the boundary of R such as $(2, 2 + L/2, z)$.

We first show that the model (2.21) exhibits a FM phase transition as T is lowered. To this end, we set $c_1 = c_3 = 0$ and $(c_2, c_4, c_5) = (0.5, 4.0, 1.0)$, and increase β in the Boltzmann factor of Eq. (2.21). In Fig. 1 we show C and m_μ . It is obvious

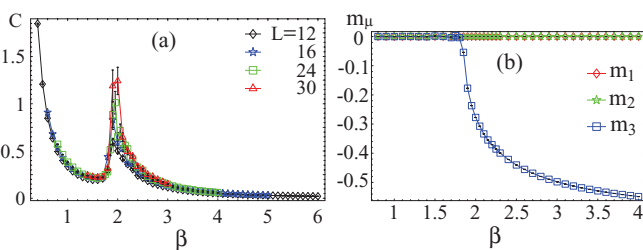


FIG. 1. (Color online) (a) Specific heat for $(c_2, c_4, c_5) = (0.5, 4.0, 1.0)$ and $c_1 = c_3 = 0$. At $\beta \simeq 2.0$, C exhibits a sharp peak indicating a second-order FM phase transition. (b) Each component of magnetization m_μ vs β . For $T < T_{\text{FM}}$, m_3 develops, whereas m_1 and m_2 are zero within the errors as expected.

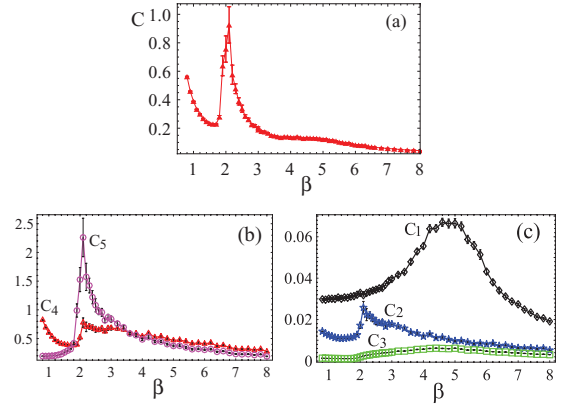


FIG. 2. (Color online) (a) Specific heat vs β for $(c_1, c_3) = (0.2, 0.2)$ and $(c_2, c_4, c_5) = (0.5, 4.0, 1.0)$ ($L = 20$). There is a large peak at $\beta \simeq 2.1$ and a small one at $\beta \simeq 4.5$. (b), (c) Specific heat C_i of each term of F in Eq. (2.21) vs β . The small and broad peak at $\beta \simeq 4.5$ in C is related to fluctuations of the c_1 term.

that a second-order phase transition to the FM state takes place at $\beta_{\text{FM}} = 1/T_{\text{FM}} \simeq 2.0$. We verified that other cases with various values of $c_{2,4,5}$ exhibit similar FM phase transitions.

Next, let us study the SC phase transition. Here, it is useful to consider the case of all $c_i = 0$ except for c_1 . Then, the model is related to the $\text{CP}^1 + \text{U}(1)$ lattice gauge theory,²³ which has the energy of the form $F_{\text{CP}^1} = -(c_1/2) \sum (\bar{z} U z + \text{c.c.}) + F_A$ where F_A is the compact version (2.4). In fact, they agree by setting $1/e^2 = 0$. The phase structure of this model is studied in Ref. 23 and it is found that the phase transition from the confinement phase to the Higgs phase takes place at $c_1 \simeq 2.85$ for $1/e^2 = 0$. Thus, the SC state exists at sufficiently large c_1 .

For simulation, we put $(c_1, c_3) = (0.2, 0.2)$ and $(c_2, c_4, c_5) = (0.5, 4.0, 1.0)$. In Fig. 2(a), we show C versus β . There is a large and sharp peak at $\beta \simeq 2.1$ and a small and broad one at $\beta \simeq 4.5$. In order to understand physical meaning of the second peak, it is useful to measure “specific heat” of each term f_i in the free energy (2.16) defined by $C_i = \langle (F'_i - \langle F'_i \rangle)^2 \rangle / L^3$. Figure 2(c) shows that the specific heat of the c_1 term has a relatively large and broad peak at $\beta \simeq 4.5$. Then, we conclude that the SC phase transition takes place at $\beta_{\text{SC}} \simeq 4.5$.

To verify this conclusion, we show $G_m(r)$ and $G_S(r)$ in Fig. 3. At $\beta = 2.5$, $G_m(r)$ exhibits a finite amount of the FM order, whereas $G_S(r)$ decreases very rapidly to vanish. This means that, as T is decreased, the FM transition takes place first and then the SC transition does. Therefore, for $\beta \geq \beta_{\text{SC}} \simeq 4.5$, the FM and SC orders coexist.

It is interesting to clarify the relation between the bare transition temperature T_{SC}^0 in Eq. (2.11) and the genuine

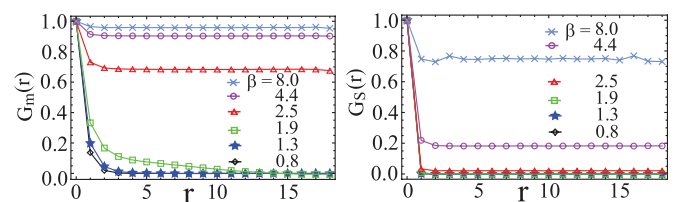


FIG. 3. (Color online) Correlation functions $G_m(r)$ and $G_S(r)$ at various T 's for $L = 20$. c_i 's are the same as in Fig. 2.

transition temperature T_{SC} . From Eq. (2.21), any physical quantity is a function of βc_i . In the numerical simulations, we fix the values of c_i and vary β as explained. Then, the result $\beta_{SC} \simeq 4.5$ means

$$\beta c_1|_{T=T_{SC}} = 4.5 \times 0.2. \quad (3.5)$$

By using Eq. (2.20), this gives the following relation:

$$\frac{1}{T_{SC}} \frac{K\alpha(T_{SC}^0 - T_{SC})a}{\lambda} = 0.90, \quad (3.6)$$

$$T_{SC} = \left(1 + \frac{0.90\lambda}{K\alpha a}\right)^{-1} T_{SC}^0.$$

Equation (3.6) shows that the transition temperature is lowered by the fluctuations of the phase degrees of freedom of Cooper pairs. We expect that a relevant contribution to lowering the SC transition temperature comes from vortices that are generated spontaneously in the FMSC as we show in Sec. III B.

After having confirmed that the genuine critical temperature can be calculated by the critical value of β with fixed c_i , we use the word temperature in the rest of the paper just as the one defined by $T \equiv 1/\beta$ while c_i are T -independent parameters.

The Meissner effect is one of the most important phenomena for a SC order. To study it, we follow the following steps:²³ (i) introduce a vector potential $A_{x\mu}^{\text{ex}}$ for an external magnetic field, (ii) couple it to Cooper pairs by replacing $U_{x\mu} \rightarrow U_{x\mu} \exp(iA_{x\mu}^{\text{ex}})$ in the c_1 term of f_x and add its magnetic term $f_x^{\text{ex}} = +c_2'(\vec{m}_x^{\text{ex}})^2$ ($c_2' > 0$) to f_x with \vec{m}_x^{ex} defined in the same way as (2.17) by using $A_{x\mu}^{\text{ex}}$, (iii) let $A_{x\mu}^{\text{ex}}$ fluctuate together with z_{xa} and $A_{x\mu}$ and measure an effective mass M_G of $A_{x\mu}^{\text{ex}}$ via the decay of correlation functions of \vec{m}_x^{ex} . The result of \vec{m}_x^{ex} propagating in the 1-2 plane is shown in Fig. 4. It is obvious that the mass M_G starts to develop at the SC phase transition point, and we conclude that the Meissner effect takes place in the SC state.

B. SC transition and vortices in a constant magnetic field

Because the observed SC state in Figs. 2 and 3 coexists with the FM order, it is expected that vortices of the SC order parameter are induced there spontaneously.²⁴ To verify this expectation, we set the vector potential $A_{x\mu}$ to a position-dependent but nonfluctuating value that corresponds to a uniform magnetic field in the third direction, and study the

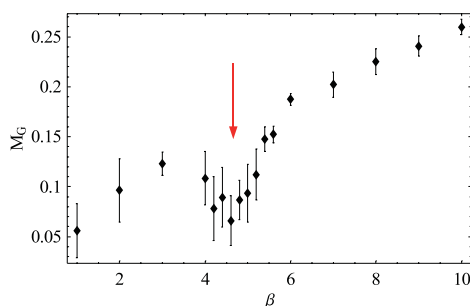


FIG. 4. (Color online) Gauge-boson mass M_G of the external magnetic field propagating in the x - y plane vs β for the same c_i as in Fig. 2 and $c_2' = 3.0$ ($L = 16$). At the SC phase transition point $\beta_{SC} \simeq 4.5$ (indicated by an arrow) determined by the peak of C_1 , M_G starts to increase from small values.

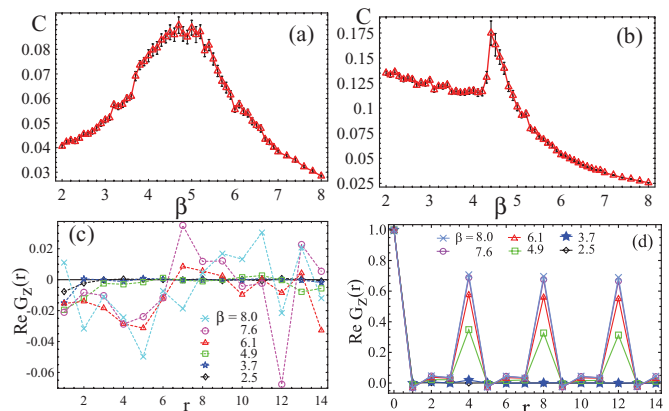


FIG. 5. (Color online) The results for a constant magnetic field $\vec{m}_x = (0, 0, m_{x3})^t$ at $c_1 = c_3 = 0.2$ ($L = 16$). (a), (b) Specific heat C and (c), (d) the real part of SC correlation function $G_z(r)$ in the 1-2 plane. (a), (c) $m_{x3} = \pi/4$ and (b), (d) $m_{x3} = \pi$.

behavior of z_{xa} itself. In this case, the free energy f_x loses the local gauge symmetry (2.19), and therefore the correlation function of z_{xa} ,

$$G_z(x - x_0) = \langle \vec{z}_x \cdot \vec{z}_{x_0} \rangle, \quad (3.7)$$

has nonvanishing values in the SC phase.

In Fig. 5, we show C and $G_z(x)$ for two cases of fixed \vec{m}_x . For the case with $\vec{m}_x = (0, 0, \frac{\pi}{4})^t$, C has a shape similar to C_1 in

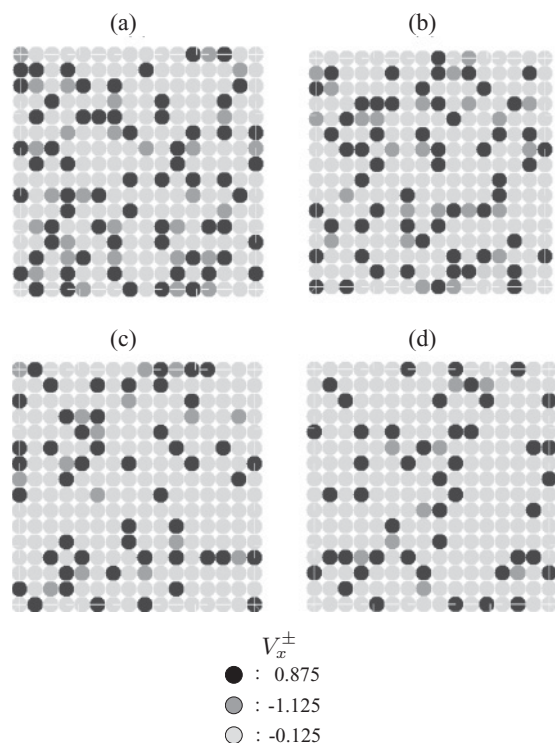


FIG. 6. Snapshots of vortex densities V_x^\pm at $c_1 = c_3 = 0.2$ for a fixed $\vec{m} = (0, 0, \pi/4)$ ($L = 16$). Black dots: $V_x^\pm = 0.875$. Dark gray dots: -1.125 . Light gray dots: -0.125 . (a) V_x^+ at $\beta = 3.0$. (b) V_x^- at $\beta = 3.0$. (c) V_x^+ at $\beta = 7.0$. (d) V_x^- at $\beta = 7.0$. The average magnitude $\langle |V_{x\pm}| \rangle$ is (a) 0.387, (b) 0.380, (c) 0.331, and (d) 0.335. The points $V_x^\pm = -0.125 = -m_3/(2\pi)$ reflect \vec{m} itself.

Fig. 2(c), and indicates a SC phase transition at $\beta \simeq 4.8$. $G_z(r)$ exhibits fluctuating behavior even for low T 's, $\beta \geq 4.9$. This suggests that vortices are spontaneously generated in the SC state violating spatial uniformity, and their locations fluctuate. In the other case of $\vec{m}_x = (0,0,\pi)^t$, C has a sharper peak at $\beta \simeq 4.5$, and $G_z(r)$ exhibits clear periodically oscillating behavior with the period $4 \times$ (lattice spacing). This implies that, in this case, locations of vortices are rather stable compared with the case of $m_{x3} = \frac{\pi}{4}$.

In order to verify the above expectation, we calculate vortex density directly. In the present model, one may define the following two kinds of gauge-invariant vortex densities V_x^+ and V_x^- in the 1-2 plane:

$$\begin{aligned} z_x^\pm &\equiv z_{x1} \pm iz_{x2} \equiv \rho_x^\pm \exp(i\theta_x^\pm), \\ V_x^\pm &\equiv \frac{1}{2\pi} [\text{mod}(\theta_{x+1}^\pm - \theta_x^\pm - A_{x1}) \\ &\quad + \text{mod}(\theta_{x+1+2}^\pm - \theta_{x+1}^\pm - A_{x+1,2}) \\ &\quad - \text{mod}(\theta_{x+1+2}^\pm - \theta_{x+2}^\pm - A_{x+2,1}) \\ &\quad - \text{mod}(\theta_{x+2}^\pm - \theta_x^\pm - A_{x2})], \end{aligned} \quad (3.8)$$

where $\text{mod}(x) \equiv \text{mod}(x, 2\pi)$. In short, V_x^\pm describes vortices of electron pairs with the amplitude $\psi_{\uparrow(\downarrow)} = \psi_1 \pm i\psi_2 \propto z_1 \pm iz_2$.

In Fig. 6, we present snapshots of V_x^\pm at $c_1 = c_3 = 0.2$ for fixed values of gauge potential $A_{x\mu}$ corresponding to a constant magnetization $\vec{m} = (0,0,\frac{\pi}{4})^t$. It shows that (i) both of the fluctuations around zero, $\langle |V_x^\pm| \rangle$, decrease as β increases, and (ii) V_x^+ has larger fluctuations than V_x^- at high T , whereas

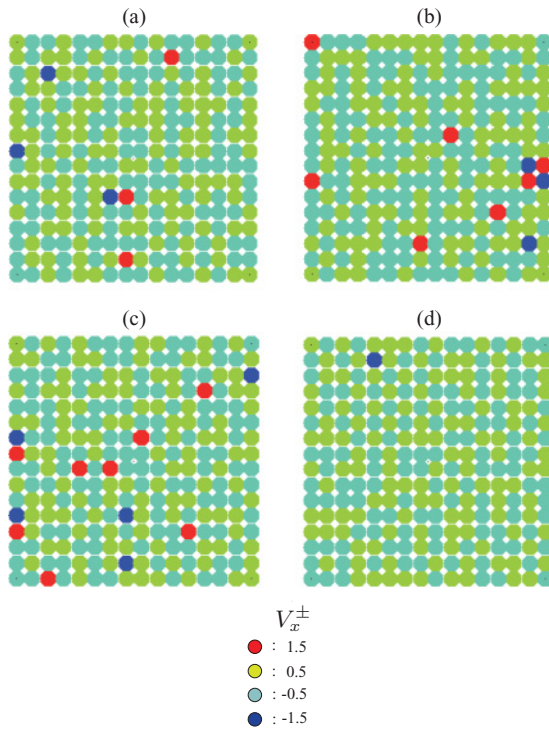


FIG. 7. (Color) Snapshots of vortex densities V_x^\pm at $c_1 = c_3 = 0.2$ for a fixed $\vec{m} = (0,0,\pi)$ ($L = 16$). (a) V_x^+ at $\beta = 3.0$. (b) V_x^- at $\beta = 3.0$. (c) V_x^+ at $\beta = 7.0$. (d) V_x^- at $\beta = 7.0$. The average magnitude $\langle |V_x^\pm| \rangle$ is (a) 0.528, (b) 0.537, (c) 0.560, and (d) 0.508. The points $V_x^\pm = -0.5 = -m_3/(2\pi)$ reflect \vec{m} itself.

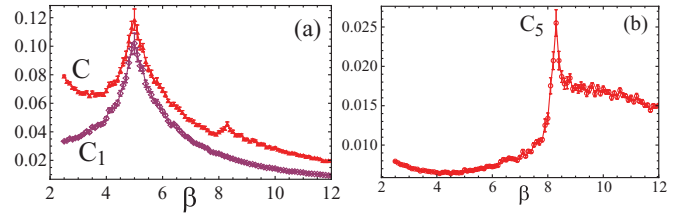


FIG. 8. (Color online) Specific heats for $c_5 = 0.4$ ($L = 12$). (a) Total C and the specific heat C_1 of the c_1 term, (b) C_5 of the c_5 term. Order of two phase transitions is interchanged ($\beta_{SC} < \beta_{FM}$).

smaller ones at low T . These behaviors are consistent with the Zeeman c_3 term in the energy f_x of Eq. (2.16), which distinguishes the z_x^+ order and the z_x^- order, and the fact that \vec{m} directs to the third direction in the present case. In Fig. 7, we also show the vortex snapshots at $c_1 = c_3 = 0.2$ and $\vec{m} = (0,0,\pi)^t$. Compared with the case $\vec{m} = (0,0,\frac{\pi}{4})^t$, vortices here are located rather systematically as we expected from the result of correlation function $G_z(r)$.

C. Order of FM and SC phase transitions and phase diagram

Let us next examine the possibility that the order of the FM and SC phase transitions are interchanged as the value of c_5 is decreased. As the c_5 term in f_x tends to align \vec{m}_x , T_{FM} decreases as c_5 is decreased. Most of the FMSC materials lose the FM order as the applied P is increased, and then it is phenomenologically expected that c_5 is a decreasing function of P . We consider several cases with $c_5 = 1.5, 1.0, 0.7, 0.5, 0.4$, and 0.3 , while other c_i are fixed to the same values as those in Fig. 2 where $c_5 = 1.0$.

We find that the order of two phase transitions actually interchanges at $c_5 \simeq 0.5$. In Fig. 8, we show the specific heat C, C_1, C_5 for $c_5 = 0.4$. C has the two peaks at $\beta_{SC} \sim 5.0 < \beta_{FM} \sim 8.3$. C_1 is sharper than in the case of $c_5 = 1.0$ in Fig. 2.

In Fig. 9, we present $G_m(r)$ and $G_S(r)$ with r in the 1-2 plane for $c_5 = 0.4$, which exhibit very peculiar behavior. In the FM and SC coexisting phases ($T < T_{FM}$), they have nonvanishing values only near the surface of the lattice in contrast with Fig. 3. This behavior survives in larger systems. For example, we define the thickness ΔL of the coexisting region such that the ordered region in the 1-2 plane occupies the interval $2 + \Delta L + (\text{disordered region}) + \Delta L + 2$ in the lattice length $2 + L + 2$ in the $\mu = 1, 2$ directions. We obtain $\Delta L \simeq 3$ for $L = 12$ (Fig. 9) and $\Delta L \simeq 4$ for $L = 16$, so about the outer half region in the linear dimension is occupied by the ordered state. This implies that the FMSC coexisting phase appears in the region including the surface of the material and not in the

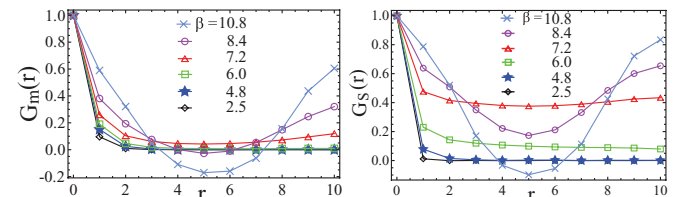


FIG. 9. (Color online) Correlation functions $G_m(r)$ and $G_S(r)$ at $c_5 = 0.4$ ($L = 12$). The other c_i are the same as those in Fig. 2. They exhibit orders near the surface of the lattice.

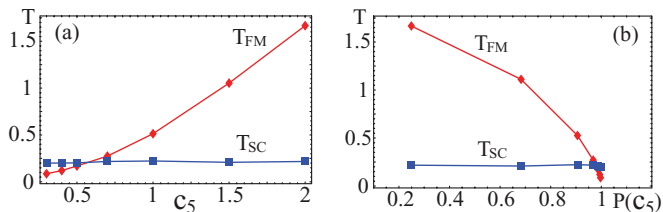


FIG. 10. (Color online) Phase diagrams in (a) c_5 - T and (b) P - T planes with $P_c = 1.0$, $c_5^* = 2.2$, and $\gamma = 3.0$ in Eq. (3.9). c_1 - c_4 are the same as in Fig. 2.

central region inside the system. We note that this “surface” region is not two dimensional but three dimensional because the SC-FM transition is a genuine second-order one, which is not allowed in a two-dimensional system.²⁵ This phenomenon is a prediction of the present model.

It is intriguing to draw a phase diagram in the P - T plane assuming certain phenomenological relation between c_5 and P . In the experiments, the critical temperature T_{FM} is a decreasing function of P . This means that the parameters c_2 , c_4 , and c_5 in Eq. (2.16) vary as functions of P . Changes of c_2 and/or c_4 influence the magnitude of the magnetization vector \vec{m}_x and result in a change of c_5 after a renormalization of \vec{m}_x . Then, for example, one may “phenomenologically” assume

$$c_5 = c_5^* \left(1 - \frac{P(c_5)}{P_c} \right)^{1/\gamma}, \quad (3.9)$$

where P_c is the critical pressure at which the FM order disappears even at $T \rightarrow 0$ (i.e., at $c_5 = 0$), c_5^* is the value of c_5 at which $P = 0$, and the power γ is a fitting parameter. In Fig. 10, we show the phase diagram drawn with certain choice of these parameters. This phase diagram has a similar structure to the experimental result of UCoGe.

In the same way as decreasing c_5 , the case of increasing c_3 has been studied with several choices of c_5 and $(c_1, c_2, c_4) = (0.2, 0.5, 4.0)$. Both T_{FM} and T_{SC} increase as c_3 increases. Furthermore, for sufficiently large values such as $c_3 = 1.5$, $T_{\text{FM}} > T_{\text{SC}}$ even for $c_5 = 0.5$ as expected. This indicates that the present model with larger c_3 may provide a phase diagram similar to that of UGe₂ and URhGe.

IV. CONCLUSION

In summary, we have proposed a GL model defined on the 3D lattice for the FMSC state, and shown that it explains some experimental observations such as the phase diagram and predicts the homogeneous and inhomogeneous FMSC states. This model naturally includes effects of topological excitations, vortices, that play an important role for the SC phase transition in the FM state. Although the obtained global phase structure is similar to that of MFT, the appearance of inhomogeneous configurations such as the FMSC state and vortex configurations are certainly beyond the scope of MFT. In the present analysis, we consider the “London limit,” in which the radial fluctuations of the two-gap SC order parameters are ignored. As we explained in Sec. II A, these fluctuations may change the order of SC phase transitions and may play an important role in SC transitions that are induced by an external magnetic field. This problem is under study and results will be reported in a future publication.

ACKNOWLEDGMENTS

We thank K. Sawamura, K. Uchida, and T. Shimizu for their collaborations in the early stage of this study. This work was partially supported by a Grant-in-Aid for Scientific Research from Japan Society for the Promotion of Science under Grants No. 20540264 and No. 23540301.

¹S. S. Saxena, P. Agarwal, K. Ahilan, F. M. Grosche, R. K. W. Haselwimmer, M. J. Steiner, E. Pugh, I. R. Walker, S. R. Julian, P. Monthoux, G. G. Lonzarich, A. Huxley, I. Sheikin, D. Braithwaite, and J. Flouquet, *Nature (London)* **406**, 587 (2000); A. Huxley, I. Sheikin, E. Ressouche, N. Kernavanois, D. Braithwaite, R. Calemczuk, and J. Flouquet, *Phys. Rev. B* **63**, 144519 (2001); N. Tateiwa, T. C. Kobayashi, K. Hanazono, K. Amaya, Y. Haga, R. Settai, and Y. Onuki, *J. Phys.: Condens. Matter* **13**, L17 (2001).

²D. Aoki, A. Huxley, E. Ressouche, D. Braithwaite, J. Floquet, J.-P. Brison, E. Lhotel, and C. Paulsen, *Nature (London)* **413**, 613 (2001).

³N. T. Huy, A. Gasparini, D. E. de Nijs, Y. Huang, J. C. P. Klaasse, T. Gortenmulder, A. de Visser, A. Hamann, T. Görlach, and H. v. Löhneysen, *Phys. Rev. Lett.* **99**, 067006 (2007).

⁴E. Slooten, T. Naka, A. Gasparini, Y. K. Huang, and A. de Visser, *Phys. Rev. Lett.* **103**, 097003 (2009).

⁵K. Machida and T. Ohmi, *Phys. Rev. Lett.* **86**, 850 (2001); M. B. Walker and K. V. Samokhin, *ibid.* **88**, 207001 (2002).

⁶V. P. Mineev, *Phys. Rev. B* **66**, 134504 (2002).

⁷For experimental evidence, see F. Hardy and A. D. Huxley, *Phys. Rev. Lett.* **94**, 247006 (2005); A. Harada, S. Kawasaki, H. Mukuda,

Y. Kitaoka, Y. Haga, E. Yamamoto, Y. Onuki, K. M. Itoh, E. E. Haller, and H. Harima, *Phys. Rev. B* **75**, 140502 (2007).

⁸The preliminary version of this work has been reported in A. Shimizu, H. Ozawa, I. Ichinose, and T. Matsui, *J. Phys.: Conf. Ser.* (to be published).

⁹V. P. Mineev and T. Champel, *Phys. Rev. B* **69**, 144521 (2004); D. V. Shopova and D. I. Uzunov, *ibid.* **79**, 064501 (2009); X. Jian, J. Zhang, Q. Gu, and R. A. Klemm, *ibid.* **80**, 224514 (2009).

¹⁰S. Coleman and E. Weinberg, *Phys. Rev. D* **7**, 1888 (1973); B. I. Halperin, T. C. Lubensky, and S. K. Ma, *Phys. Rev. Lett.* **32**, 292 (1974).

¹¹K. Kajantie, M. Karjalainen, M. Laine, and J. Peisa, *Phys. Rev. B* **57**, 3011 (1998), and references cited therein.

¹²K. Kajantie, M. Laine, T. Neuhaus, A. Rajantie, and K. Rummukainen, *Nucl. Phys. Proc. Suppl.* **106**, 959 (2002).

¹³M. Chavel, *Phys. Lett. B* **378**, 227 (1996).

¹⁴M. B. Einhorn and R. Savit, *Phys. Rev. D* **17**, 2583 (1978); **19**, 1198 (1979).

¹⁵K. G. Wilson, *Phys. Rev. D* **10**, 2445 (1974); A. M. Polyakov, *Phys. Lett. B* **59**, 82 (1975).

- ¹⁶S. Wenzel, E. Bittner, W. Janke, A. M. J. Schakel, and A. Schiller, *Phys. Rev. Lett.* **95**, 051601 (2005).
- ¹⁷D. J. E. Callaway and L. J. Carson, *Phys. Rev. D* **25**, 531 (1982).
- ¹⁸T. Ono, S. Doi, Y. Hori, I. Ichinose, and T. Matsui, *Ann. Phys. (NY)* **324**, 2453 (2009).
- ¹⁹E. Smørgrav, J. Smiseth, E. Babaev, and A. Sudbø, *Phys. Rev. Lett.* **94**, 096401 (2005), and references cited therein.
- ²⁰N. T. Huy, D. E. de Nijs, Y. K. Huang, and A. de Visser, *Phys. Rev. Lett.* **100**, 077002 (2008).
- ²¹We have included the charge $-2e$ in $A_{x\mu}$.
- ²²See, e.g., J. Zinn-Justin, *Quantum Field Theory and Critical Phenomena* (Clarendon, Oxford, 1993).
- ²³S. Takashima, I. Ichinose, and T. Matsui, *Phys. Rev. B* **72**, 075112 (2005).
- ²⁴T. Ohta, T. Hattori, K. Ishida, Y. Nakai, E. Osaki, K. Deguchi, N. K. Sato, and I. Satoh, *J. Phys. Soc. Jpn.* **79**, 023707 (2010); K. Deguchi, E. Osaki, S. Ban, N. Tamura, Y. Simura, T. Sakakibara, I. Satoh, and N. K. Sato, *ibid.* **79**, 083708 (2010).
- ²⁵N. D. Mermin and H. Wagner, *Phys. Rev. Lett.* **17**, 1133 (1966); P. C. Hohenberg, *Phys. Rev.* **158**, 383 (1967); S. Coleman, *Commun. Math. Phys.* **31**, 259 (1973).